Proceedings of the ASME 2018 International Mechanical Engineering Congress and Exposition
IMECE2018
November 9-15, 2018, Pittsburgh, PA, USA

IMECE2018-86965

MOLECULAR DYNAMICS SIMULATION OF EXPLOSIVE BOILING ON CONCAVE NANOSTRUCTURED SURFACE

Pengfei Ji, Mengzhe He and **Yiming Rong**
Shenzhen Key Laboratory for Additive Manufacturing of High-performance Materials
Department of Mechanical and Energy Engineering
Southern University of Science and Technology
Shenzhen 518055, China
E-mail: pengfeiji2htec@outlook.com

Yuwen Zhang
Department of Mechanical and Aerospace Engineering
University of Missouri
Columbia MO 65211, USA

Yong Tang
Key Laboratory of Surface Functional Structure Manufacturing of Guang Dong Higher Education Institutes
School of Mechanical and Automotive Engineering
South China University of Technology
Guangzhou 510640, China

ABSTRACT

Explosive boiling occurs when a liquid film contacts with the wall at extremely high temperature, which is detrimental to continuous heat transfer process. In this paper, five kinds of nanostructured surfaces with equal distance between neighboring nano-concaves and flat surface are set up to study the explosive boiling of liquid argon on copper surface. For all the five cases with concave nanostructured surface, the ratio of concave nanostructured surface area to flat surface area is kept as a constant. The temporal and spatial distributions of temperature, atomic motion and number density are recorded to study the effects of different nanostructured surface designs on explosive boiling. From the perspective of reducing explosive boiling, the most favorable nanostructured surface is determined.

KEYWORDS

Explosive Boiling; Nanostructured Surface; Superheating.

INTRODUCTION

As an effect way to convey thermal energy from the material surface to liquid, boiling is crucially important in thermal management. If the temperature difference between liquid and material surface causes the liquid temperature to be slightly higher than the boiling point, thermal energy is transferred from material surface to liquid via heterogeneously steady boiling. However, if the temperature difference is sufficiently large to induce the liquid temperature much higher than the boiling point at short time, a vapor film forms between material surface and liquid. Comparing with liquid, vapor film carries much less thermal energy from hot material surface, which results in the burnout of material surface. If the temperature of material surface is above 90% of the critical temperature of liquid, the liquid contacting with material surface becomes superheated in terms of homogenous nucleation of vapor bubble [1,2]. The superheated liquid is metastable, which further explodes and transforms into a stable liquid-vapor state. As a consequence, explosive boiling pushes working fluid (mixture of liquid and vapor) moving away from material surface directly and terminates the subsequent heat transfer process.

Considerable attentions have been drawn to study the explosive boiling. By heating a tungsten wire at rapid speed up to $5 \times 10^5\ K/s$, the transition between nucleate and film boiling was studied by Fau *et al*. [3]. Nevertheless, the transient heat transfer coefficient was not measured due to the difficulty of characterizing vapor wave. A model for boiling explosion during rapid liquid heating was proposed by Hassan *et al.* [4]. Good agreement between the result from theoretical model and that from experiment was reached. Moreover, as pointed out by Hassan *et al.* [4], the liquid might be heated to much higher temperature before theoretical boiling explosion. The explosive boiling of heated water emulsion droplets was studied by Volkov

and Strizhak [5]. A non-linear increase of evaporation rate was found during the disintegration process of droplet. By setting up different forms of surface, the pool boiling of acetone on an aluminum surface was studied by Masri *et al.* [6]. It was found that ultra-smooth surface with a small number of defects brought the best thermal characteristics at high heat flux.

From the perspective of boiling at different length scales, the macroscopic description of continuum liquid film on material surface becomes questionable at nanoscale regime [7]. Since the miniaturized size of liquid film, the interfacial thermal resistance between liquid and material surface at nanoscale is different from that at macroscale. Up to now, the experimental instruments still cannot reach the ultrashort time scale of explosive boiling. Additionally, the macroscopic description of continuum liquid film on material surface becomes questionable at nanoscale regime [7]. Molecular dynamics (MD) simulation has the advantage of capturing detailed information on atomic motion. For a system containing thousands to millions of atoms, the explosive boiling process can be simulated. The homogeneous nucleation of water and liquid nitrogen was studied by Zou *et al.* [8]. Since the strong interaction forms of hydrogen bond, water was found tougher to produce bubble nucleus, which further led to higher energy conversion ratio in liquid nitrogen than that in water. The explosive boiling of water on hot copper plate was simulated by Mao *et al.* [9]. The results showed a non-vaporization molecular layer staying on the hot plate surface, even though the surface temperature was much higher than the critical point of water. By setting hydrophilic, hydrophobic and neutral properties of material surface for explosive boiling, hydrophobic surface was found the best to reduce explosive boiling [10]. Moreover, with the advancement of nanotechnology, different kinds of nanostructures were placed on flat material surface to probe their effects on explosive boiling [11–16]. Nevertheless, to the best of authors' knowledge, there is no work focusing on explosive boiling of liquid film on nanostructured surface generated by laser drilling and micro-cutting of flat surface. In other words, the available work in literature focuses on nanostructures added on the flat material surface, rather than subtracted from flat material surface.

In this paper, five kinds of concave nanostructured surfaces with equal distance between neighboring nano-concaves are designed. The same surface area ratios for five nanostructured surfaces are designed. Namely, the same area of thermal contact between liquid and material surface is kept. For comparison, the case with explosive boiling on flat surface is studied as well. The effects of nanostructured surfaces on the thermophysical characteristics of explosive boiling are investigated.

NOMENCLATURE

A	Area, nm^2
d	Depth, nm
ϵ	Depth of potential well, eV
H	Height, nm
L	Length, nm
N	Integer number
r	Radius, nm
ρ	Number density, $1/A^3$
R	Radius, nm
S	Laser intensity, W/m^3
t	Time, ns
T	Temperature, K
σ	Characteristic length, nm
W	Width, nm

MODELING AND SIMULATION

Fig. 1 Sliced view of the computational domain.

The MD simulation system was modeled with $W = 77.41\ nm$ in the x-direction, $H = 8.68\ nm$ in the y-direction and $L = 8.68\ nm$ in the z-direction. Figure 1 shows the orthogonal view of the $x-y$ plane sliced at half z. Periodic boundary conditions were imposed in the y- and z-directions during MD simulation.

As seen in Fig. 1, from the left side to the right side, there are eight groups of atoms, consisting of the left fixed wall, the heat source wall, the left heat conduction wall, the liquid, the vapor, the right heat conduction wall, the heat sink wall and the right fixed wall, respectively. The walls are copper, which has a lattice constant of $0.36\ nm$. The corresponding mass density of copper is $8.96\ g/cm^3$. The liquid and vapor are argon at $90\ K$ and $1.34\ bar$, which correspond to densities $1.38\ g/cm^3$ and $7.54 \times 10^{-3}\ g/cm^3$, respectively [17]. For convenience, the mixture of liquid and vapor argon is named as working fluid. The width of left (right) fixed wall is $0.36\ nm$. The fixed wall is used to prevent atoms from moving out of the simulation domain. The left (right) heat source (sink) wall has a width of $1.08\ nm$. The heat source is used to supply thermal energy to the simulation domain. On the contrary, the heat sink is designed to let the thermal energy flow out from the simulation domain. The left (right) heat conduction wall with a width of $1.8\ nm$ is used as interaction surface between heat source (sink) and working fluid. Widths of liquid region and vapor region are $5.78\ nm$ and $65.56\ nm$. The large enough space of vapor region allows full development and propagation of superheating working fluid during explosive boiling.

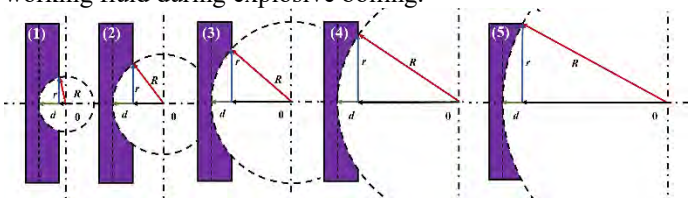

Fig. 2 Sliced view of the five concave nanostructured surface.

Five kinds of concave nanostructured surface are designed on the left heat conduction surface, which are shown in Fig. 2. Due to the periodic boundary conditions in the y- and z-directions, the neighboring nano-concaves with equal distance form an uniform pattern. The depth d of concave nanostructure is fixed

as a constant for all the five cases in Fig. 2. For the case of flat surface on left heat conduction wall, the interfacial area between the left heat conduction surface and the liquid is

$$A_{Flat} = H^2 \tag{1}$$

In addition, the curved surface area of spherical cap is

$$A_{Curve} = 2\pi Rd \tag{2}$$

The bottom area of spherical cap is

$$A_{Bottom} = \pi r^2 \tag{3}$$

Therefore, the interfacial area between the right side of the left heat conduction surface and the liquid is

$$\begin{aligned} A_{Surface} &= A_{Flat} + A_{Curve} - A_{Bottom} \\ &= H^2 + 2\pi Rd - \pi r^2 \end{aligned} \tag{4}$$

According to the Pythagorean theorem

$$R^2 = r^2 + (R - d)^2 \tag{5}$$

Therefore, Eq. (4) becomes

$$A_{Surface} = H^2 + \pi d^2 \tag{6}$$

which means $A_{Surface}$ is independent of R and r. In other words, once d is fixed, the areas of heat conduction surface for the five cases in Fig. 2 are the equal. It eliminates the factor of different areas of thermal communication between conduction wall and liquid. Table 1 lists the radius R for concave nanostructures and their volumes V. The case with flat surface on left heat conduction wall is named as case 0. Cases 1-5 correspond to the five cases shown in Fig. 2. The diameter of the nanostructured surface for Case 5 is almost equal to the entire widths of simulation domain in the y- and z-directions. Nevertheless, there are still flat surfaces existing at the four edges of the nanostructured surface, which occupy 22.18% of the interfacial area between right side of left heat conduction surface and liquid region.

Table 1 Geometric Parameters for the Six Cases

Case Number	r (nm)	R (nm)
0	0	0
1	1.44	1.5
2	2.16	2.7
3	2.88	4.38
4	3.6	6.54
5	4.32	9.18

The atomic interactions between argon and argon, argon and copper, copper and copper are described by Lennard-Jones potential E, which is expressed in the following equation

$$E = 4\epsilon\left[\left(\frac{\sigma}{r}\right)^{12} - \left(\frac{\sigma}{r}\right)^{6}\right] \tag{7}$$

where r is the distance between two atoms, ϵ is the depth of potential well. The interatomic potential becomes zero when r is equal to σ.

The Lorentz-Berthelot combination rule is implemented to obtain potential depth and characteristic length between argon and copper [18], namely

$$\begin{cases} \epsilon_{Ar-Cu} = \sqrt{\epsilon_{Ar}\epsilon_{Cu}} \\ \sigma_{Ar-Cu} = (\sigma_{Ar} + \sigma_{Cu})/2 \end{cases} \tag{8}$$

The entire simulation was divided into three stages. Stage 1 was for thermal preparation at constant temperature. The Berendsen thermostat [17] was applied to keep the heat source wall, the working fluid (liquid and vapor) and the heat sink wall with temperatures at $250\ K$, $90K$ and $90\ K$, respectively. The thermostat worked on translational degrees of freedom for atoms by rescaling their velocity every time step. The left and right heat conduction walls were set as thermal insulators to impede thermal energy transport between its neighboring walls. After running for $0.05\ ns$, well thermal equilibrium reached for the three regions maintained by Berendsen thermostat. Subsequently, Stage 2 started by releasing thermostat to let the entire system run in terms of micro-canonical ensemble. Stage 2 lasted for $0.1\ ns$. By shifting the left and right heat conduction walls from thermal insulation to thermal conducting media, Stage 3 started and lasted from $1\ ns$. The combined group of heat conduction walls and working fluid were simulated in terms of micro-canonical ensemble, while the heat source wall and heat sink wall were simulated in terms of separate canonical ensembles. The Nosé-Hoover thermostat [19] was implemented in the canonical ensemble simulation, which updated the atomic position and velocity every time step. The MD simulation was carried out under the framework of LAMMPS [20] program.

It is worth noting the information on atomic motion during the entire simulation process. For the group of atoms in the left and right fixed walls, the atomic velocities were set as zero to prevent atoms from moving out of the simulation domain. For the group of atoms in the left heat source wall and the right heat sink wall, the atoms vibrate around their initial positions, which maintains the walls at solid state. For the group of atoms in the left and right heat conduction walls, the atoms were fixed at zero velocity to play the role of thermal insulator at Stages 1 and 2. However, at Stage 3, the atoms in the left and right heat conduction walls were allowed to vibrate like those in the left heat source wall and the right heat sink wall, which conduct heat from the heat source wall to the working fluid and from the working fluid to the heat sink wall.

RESULTS AND DISCUSSION

As seen in Fig. 3, right after releasing the thermal insulation of heat conduction wall, the average temperature of working fluid is heated above the critical point $150.86\ K$ of argon [21]. Due to the separation of working fluid from the concave nanostructured surface and the local thermal expansion of superheated liquid cluster, the temperature of working fluid T_{WF} presents steep decrease from $0.006\ ns$ to $0.015\ ns$. Moreover, as seen in the inset of Fig. 3, due to the occurrence of explosive boiling in ultrashort time (less than $10\ ps$), the abruptly increased pressure in the enclosed space of simulation domain induces sharp temperature increase of heat sink wall T_{Sink}. However, the efficient temperature of Nosé-Hoover thermostat balances the increased T_{Sink} soon.

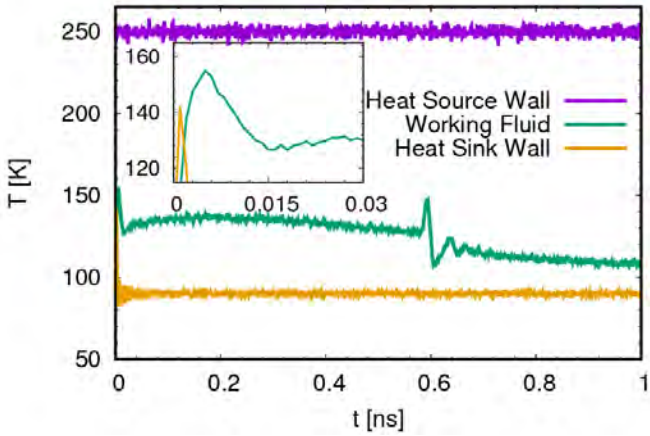

Fig. 3 The temporal evolution of temperatures T for heat source wall, working fluid and heat sink wall for Case 3.

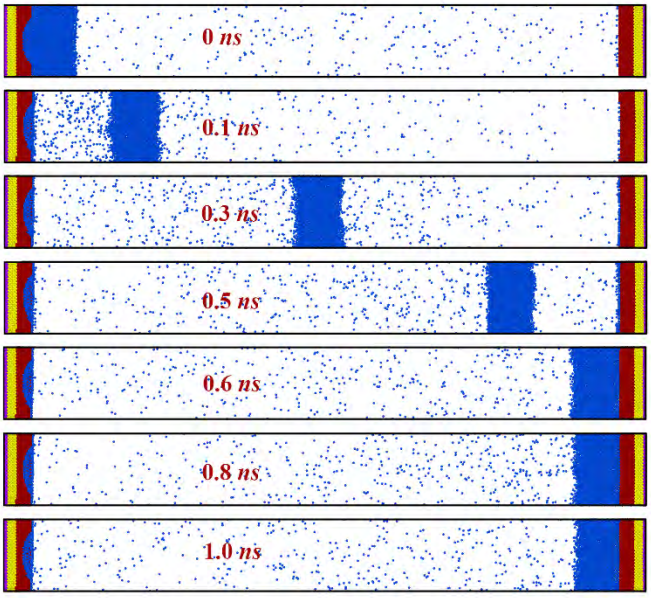

Fig. 4 Snapshots of atomic motion for Case 3.

A zigzag profile of T_{WF} is seen from $0.56\ ns$ to $0.64\ ns$. Combing with the snapshots of atomic motion for Case 3 shown in Fig. 4, it can be seen the atomic cluster induced by explosive boiling has arrived the right heat conduction wall at $0.6\ ns$. For the argon atoms having arrived and stopped on the surface of the right heat conduction wall, the transient compression imposed by the remained proportion of atoms (still at high speed motion from left to right) and the fixed heat conduction wall, results in conversion of atomic potential energy to internal kinetic energy. Therefore, the abrupt increment of T_{WF} is caused by collision of the atomic argon cluster with the right heat conduction wall. In addition, as seen in the concave nanostructured surface in Fig. 4, even though the explosive boiling happens, there are still a small number of argon atoms adhering on the surface of the left heat conduction wall. Since the strong interatomic force exists between argon (in liquid layer) and copper (in heated wall), a non-evaporating thin liquid layer is observed on the heated surface throughout the simulation. The same kind of results has been numerically and experimentally find elsewhere [22,23].

After quantitatively counting the number of atoms in the non-evaporating thin layer adhering on the surface of the left heat conduction wall, the numbers are 1235 for Case 0, 1257 for Case 1, 1132 for Case 2, 1165 for Case 3, 1084 for Case 4 and 1144 for Case 5. Even though the surface areas are the same for the six cases, it can be found that Case 4 has the smallest number of non-evaporating argon atoms. Except for Case 1, the other concave nanostructured surfaces cause smaller number of non-evaporating argon atoms. By arranging the sequence of Cases 0-5 according to the ascending number of non-evaporating argon atoms for each cases, it can be found the sequence qualitatively agrees with the sequence of atomic cluster arriving to right heat conduction wall (seen in Fig. 5). Therefore, it can be concluded that the slower detachment of atomic cluster from the left heat conduction wall, the smaller number of non-evaporating argon atoms adhering on left heat conduction wall.

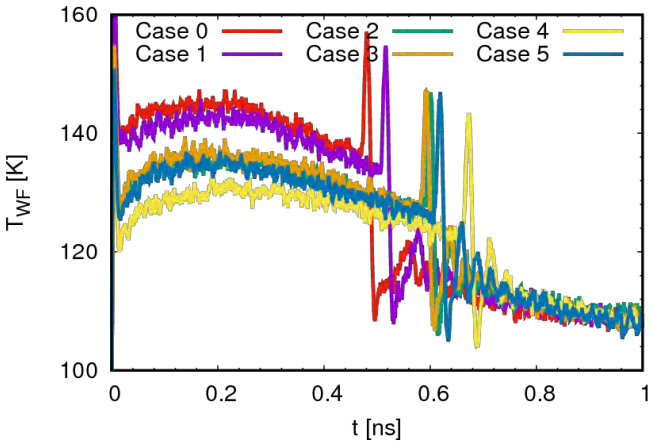

Fig. 5 The temporal evolution of temperature of working fluid T_{WF} for the cases with explosive boiling on concave nanostructured surface and flat surface.

Subsequently, according to the law of conservation of momentum, the right heat conduction wall exerts a force from right to left, the atomic cluster is bounced back with volume expansion, as a result of T_{WF} decrease from $\sim 150\ K$ to $\sim 120\ K$. Nevertheless, the high pressure (induced by explosive boiling) in left side the atomic cluster prevents the atomic cluster

from moving to the left direction, which further keeps the atomic cluster on right heat conduction wall. The damping oscillation of several T_{WF} peaks and valleys reflects the cycles of compression and expansion. Since the heat sink extracts thermal energy from atomic cluster, T_{WF} still shows decreasing trend at the end of simulation. The limit of T_{WF} after infinite long time should be equal to T_{Sink}.

The temporal evolution of T_{WF} for the five cases in Fig. 2 and the case with flat surface on left heat conduction wall (Case 0) are plotted in Fig. 5. Due to the smooth flat surface for Case 0, the highest T_{WF} is seen for Case 0 after explosive boiling. It is worth noting that Case 4 has the lowest T_{WF}. Therefore, the case with $R = 6.54\ nm$ is a turning point, where the explosive boiling is least intensive. A fast increase for the degree of the explosive boiling is seen when R increase from $1.5\ nm$ to $2.7\ nm$. It is true that the number of argon atoms adsorbed on right heat conduction wall is significantly less than that of argon atoms in atomic cluster (film). The adsorption is because of strong interatomic force existing between argon atom (in liquid layer) and copper atom (in heated wall). The remained argon atoms beyond the interaction distance between argon atom and copper atom are not adsorbed on the right heat conduction wall. Nevertheless, these argon atoms in the atomic cluster still at high traveling speed from left to right. The compression accumulates until all of the argon atoms in the left side of atomic cluster stop moving from left to right, which results in $\sim 20\ K$ increase of the working fluid temperature T_{WF}. There are no significant differences among T_{WF} for Cases 2, 3 and 5. The final T_{WF} for all the six cases get converged to $110\ K$, indicating the effect of nanostructured surface no longer works.

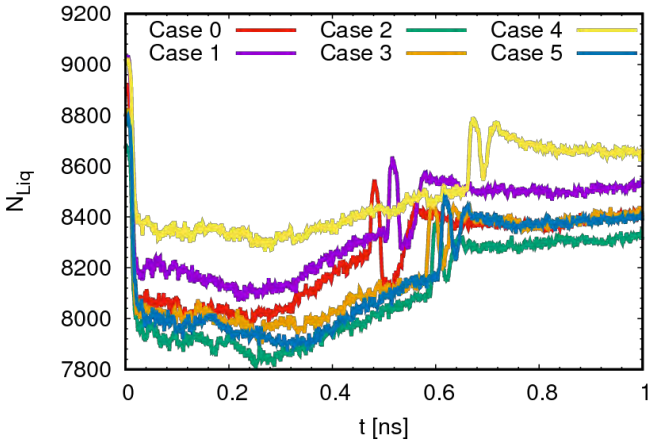

Fig. 6 The temporal evolution of number of liquid argon atoms N_{Liq} for the cases with explosive boiling on concave nanostructured surface and flat surface.

As seen in Fig. 6, accompanying with the triggered explosive boiling, the number of liquid argon atoms N_{Liq} reduces greatly. The judgement of whether an argon atom belongs to liquid or vapor depends on the number of neighboring atoms with a certain threshold distance. As calculated from [24], the threshold $0.53\ nm$ and the number of atoms 7 are chosen. In other words, if an argon atom has more than 7 atoms within the distance $0.53\ nm$ from it, the atom is counted as liquid atom. Otherwise, it is vapor atom. With N_{Liq} continues decrease to $\sim 0.26\ ns$, the minimum N_{Liq} is achieved for all the six cases. Subsequently, with the progress of simulation, N_{Liq} gradually increases, until the atomic cluster of argon atoms arrive to right heat conduction wall. The damping oscillation of N_{Liq} agrees with the damping oscillation of T_{WF}. Since the heat sink plays the role of cooling down heated argon atoms, N_{Liq} still shows gentle increasing tendency after the atomic cluster arriving to the right heat conduction wall.

CONCLUSIONS

Explosive boiling of liquid argon on concave nanostructured surface and flat surface is studied in this paper. By capturing the temporal evolution of temperature of working fluid (mixture of liquid and vapor argon), explosive boiling is observed once the liquid argon contacts with the heat conduction wall at $250\ K$. Comparing with the flat surface, the concave nanostructured design reduces degree of superheating and speed of atomic cluster after explosive boiling. The design of Case 4 has the best performance to resist explosive boiling. Other design of nanostructured surface, such as the grooved surface remains to be explored in the future work.

ACKNOWLEDGMENTS

Support for this work by the National Natural Science Foundation of China under grant numbers 51705234, U1537202 and 2015B010132005, the Shenzhen Key Laboratory for Additive Manufacturing of High-performance Materials under grant number ZDSYS201703031748354, the Southern University of Science and Technology Presidential Postdoctoral Fellowship and the projected funded by China Postdoctoral Science Foundation under grant number 2017M612653 are gratefully acknowledged.

REFERENCES

[1] Fucke, U. S. and W., 1978, "Experimental Determination of Critical Data of Liquid Molybdenum," J. Phys. F Met. Phys., **8**(7), p. L157.

[2] Martynyuk, M. M., 1977, "Phase Explosion of a Metastable Fluid," Combust. Explos. Shock Waves, **13**(2), pp. 178–191.

[3] Fau, S., Bergez, W., and Colin, C., 2017, "Transition between Nucleate and Film Boiling in Rapid Transient Heating," Exp. Therm. Fluid Sci., **83**, pp. 118–128.

[4] Hasan, M. N., Monde, M., and Mitsutake, Y., 2011, "Model for Boiling Explosion during Rapid Liquid Heating," Int. J. Heat Mass Transf., **54**(13), pp. 2844–2853.

[5] Volkov, R. S., and Strizhak, P. A., 2018, "Using Planar Laser Induced Fluorescence to Explore the Mechanism of the Explosive Disintegration of Water Emulsion Droplets Exposed to Intense Heating," Int. J. Therm. Sci., **127**, pp. 126–141.

[6] Al Masri, M., Cioulachtjian, S., Veillas, C., Verrier, I.,

Jourlin, Y., Ibrahim, J., Martin, M., Pupier, C., and Lefèvre, F., 2017, "Nucleate Boiling on Ultra-Smooth Surfaces: Explosive Incipience and Homogeneous Density of Nucleation Sites," Exp. Therm. Fluid Sci., **88**, pp. 24–36.

[7] Nagayama, G., Kawagoe, M., Tokunaga, A., and Tsuruta, T., 2010, "On the Evaporation Rate of Ultra-Thin Liquid Film at the Nanostructured Surface: A Molecular Dynamics Study," Int. J. Therm. Sci., **49**(1), pp. 59–66.

[8] Zou, Y., Huai, X., and Lin, L., 2010, "Molecular Dynamics Simulation for Homogeneous Nucleation of Water and Liquid Nitrogen in Explosive Boiling," Appl. Therm. Eng., **30**(8–9), pp. 859–863.

[9] Mao, Y., and Zhang, Y., 2014, "Molecular Dynamics Simulation on Rapid Boiling of Water on a Hot Copper Plate," Appl. Therm. Eng., **62**(2), pp. 607–612.

[10] Hens, A., Agarwal, R., and Biswas, G., 2014, "Nanoscale Study of Boiling and Evaporation in a Liquid Ar Film on a Pt Heater Using Molecular Dynamics Simulation," Int. J. Heat Mass Transf., **71**, pp. 303–312.

[11] Nagayama, G., Kawagoe, M., Tokunaga, A., and Tsuruta, T., 2010, "On the Evaporation Rate of Ultra-Thin Liquid Film at the Nanostructured Surface: A Molecular Dynamics Study," Int. J. Therm. Sci., **49**(1), pp. 59–66.

[12] Zhang, S., Hao, F., Chen, H., Yuan, W., Tang, Y., and Chen, X., 2017, "Molecular Dynamics Simulation on Explosive Boiling of Liquid Argon Film on Copper Nanochannels," Appl. Therm. Eng., **113**, pp. 208–214.

[13] Reza Seyf, H., and Zhang, Y., 2013, "Molecular Dynamics Simulation of Normal and Explosive Boiling on Nanostructured Surface," J. Heat Transfer, **135**(12), p. 121503.

[14] Seyf, H. R., and Zhang, Y., 2013, "Effect of Nanotextured Array of Conical Features on Explosive Boiling over a Flat Substrate: A Nonequilibrium Molecular Dynamics Study," Int. J. Heat Mass Transf., **66**, pp. 613–624.

[15] Fu, T., Mao, Y., Tang, Y., Zhang, Y., and Yuan, W., 2016, "Effect of Nanostructure on Rapid Boiling of Water on a Hot Copper Plate: A Molecular Dynamics Study," Heat Mass Transf. und Stoffuebertragung, **52**(8), pp. 1469–1478.

[16] Fu, T., Mao, Y., Tang, Y., Zhang, Y., and Yuan, W., 2015, "Molecular Dynamics Simulation on Rapid Boiling of Thin Water Films on Cone-Shaped Nanostructure Surfaces," Nanoscale Microscale Thermophys. Eng., **19**(1), pp. 17–30.

[17] 1972, "Table 1 - SATURATION LINE: TEMPERATURE BT - International Thermodynamic Tables of the Fluid State, Argon, 1971," Butterworth-Heinemann, pp. 23–24.

[18] Li, L., Ji, P., and Zhang, Y., 2016, "Molecular Dynamics Simulation of Condensation on Nanostructured Surface in a Confined Space," Appl. Phys. A, **122**(5), p. 496.

[19] Ji, P., Zhang, Y., and Yang, M., 2013, "Structural, Dynamic, and Vibrational Properties during Heat Transfer in Si/Ge Superlattices: A Car-Parrinello Molecular Dynamics Study," J. Appl. Phys., **114**(23), p. 234905.

[20] Plimpton, S., 1995, "Fast Parallel Algorithms for Short – Range Molecular Dynamics," J. Comput. Phys., **117**(June 1994), pp. 1–19.

[21] 1972, "1 - The Constituent Tables BT - International Thermodynamic Tables of the Fluid State, Argon, 1971," Butterworth-Heinemann, pp. 1–8.

[22] Yu, J., and Wang, H., 2012, "A Molecular Dynamics Investigation on Evaporation of Thin Liquid Films," Int. J. Heat Mass Transf., **55**(4), pp. 1218–1225.

[23] Mehrizi, A. A., and Wang, H., 2018, "Evaporation-Induced Receding Contact Lines in Partial-Wetting Regime on a Heated Substrate," Int. J. Heat Mass Transf., **124**, pp. 279–287.

[24] Maroo, S. C., and Chung, J. N., 2008, "Molecular Dynamic Simulation of Platinum Heater and Associated Nano-Scale Liquid Argon Film Evaporation and Colloidal Adsorption Characteristics," J. Colloid Interface Sci., **328**(1), pp. 134–146.